Published in final edited form as:
J Immunol. 2012 September 1; 189(5): 2597–2605. doi:10.4049/jimmunol.1201272.

Resolvin D1 and Resolvin D2 Govern Local Inflammatory Tone in Obese Fat1

Joan Clària[2], **Jesmond Dalli**, **Stephanie Yacoubian**, **Fei Gao**, and **Charles N. Serhan**[3]
Center for Experimental Therapeutics and Reperfusion Injury, Department of Anesthesiology, Perioperative and Pain Medicine, Brigham and Women's Hospital and Harvard Medical School, Boston, Massachusetts 02115

Abstract

The unprecedented rise in the prevalence of obesity and obesity-related disorders is causally linked to a chronic state of low-grade inflammation in adipose tissue. Timely resolution of inflammation and return of this tissue to homeostasis are key to reducing obesity-induced metabolic dysfunctions. Here, with inflamed adipose, we investigated the biosynthesis, conversion and actions of Resolvin (Rv) D1 and RvD2, potent anti-inflammatory and pro-resolving lipid mediators (LM), and their ability to regulate monocyte interactions with adipocytes. LM-metabololipidomics identified RvD1 and RvD2 from endogenous sources in human and mouse adipose tissues. We also identified pro-resolving receptors (i.e. ALX/FPR2, ChemR23 and GPR32) in these tissues. Compared to lean tissue, obese adipose showed a deficit of these endogenous anti-inflammatory signals. With inflamed obese adipose tissue, RvD1 and RvD2 each rescued impaired expression and secretion of adiponectin in a time- and concentration-dependent manner while decreasing pro-inflammatory adipokine production including leptin, TNFα, IL-6 and IL-1β. RvD1 and RvD2 each reduced MCP-1 and leukotriene B_4-stimulated monocyte adhesion to adipocytes and their transadipose migration. Adipose tissue rapidly converted both resolvins to novel oxo-resolvins. RvD2 was enzymatically converted to 7-oxo-RvD2 as its major metabolic route that retained adipose-directed RvD2 actions. These results indicate, in adipose, D-series resolvins (RvD1 and RvD2) are potent pro-resolving mediators that counteract both local adipokine production and monocyte accumulation in obesity-induced adipose inflammation.

INTRODUCTION

Expansion of adipose tissue mass in obesity is causally linked to a chronic state of "low-grade" inflammation driven by infiltrated macrophages in this tissue (1–5). The presence of increased numbers of macrophages forming characteristic "crown-like structures" that surround necrotic adipocytes and scavenge adipocyte debris is a prevalent pathological trait

[1]This work was supported in part by National Institutes of Health (grants no. P01GM095467 and R01-GM038765 to C.N.S.) and Spanish Health, Science and Innovation Ministries (grants no. SAF09/08767 and BA10/00036 to J.C.). J.C. received support from the Spanish Association for the Study of Liver Diseases (AEEH, Beca Hernández-Guío).

[3]Corresponding Author: Prof. Charles N. Serhan, Director, Center for Experimental Therapeutics and Reperfusion Injury, Department of Anesthesiology, Perioperative and Pain Medicine, Brigham and Women's Hospital, Harvard Institutes of Medicine, 77 Avenue Louis Pasteur, Boston, MA 02115, Tel: 617-525-5001, Fax: 617-525-5017, cnserhan@zeus.bwh.harvard.edu.
[2]On sabbatical from Department of Biochemistry and Molecular Genetics and Department of Physiological Sciences I, Hospital Clínic, University of Barcelona, Barcelona, Spain (jclaria@clinic.ub.es).

DISCLOSURES

CNS is an inventor on patents [resolvins] assigned to BWH and licensed to Resolvyx Pharmaceuticals. CNS is a scientific founder of Resolvyx Pharmaceuticals and owns equity in the company. CNS' interests were reviewed and are managed by the Brigham and Women's Hospital and Partners HealthCare in accordance with their conflict of interest policies. The other authors declare no competing financial interests.

in obesity (6). Although enlarged adipocytes were initially thought to be the cellular source of pro-inflammatory mediators in obesity, it was later established that the presence of infiltrated macrophages in inflamed fat perpetuates a vicious cycle of monocyte recruitment and exacerbated production of pro-inflammatory adipokines (4–6). This persistent state of inflammation, also known as "metabolic-triggered inflammation" or "metainflammation" in adipose tissue is deleterious, increasing the incidence of metabolic syndrome and obesity-related co-morbidities including dyslipidemia as well as several forms of cardiovascular disease (1–3). The key sequela of adipose tissue inflammation is insulin resistance leading to type 2 diabetes and non-alcoholic fatty liver disease (1–3).

Prolonged, unremitting inflammation in adipose tissue has a negative impact on insulin-sensitive tissues; hence, its timely resolution could be a critical step toward regaining metabolic balance. Resolvins (Rv)4 and protectins are the first pro-resolving mediators biosynthesized from essential n-3 fatty acids that stimulate active resolution of acute inflammation and return to homeostasis (7, 8). Unlike their precursors docosahexaenoic acid (DHA) and eicosapentaenoic acid (EPA), resolvins exert potent actions in the pico- to nano-molar range, e.g. counter-regulating pro-inflammatory signaling pathways and acting as "braking signals" of the persistent vicious cycle leading to unremitting inflammation (for a review, see ref. 8). These endogenous autacoids show remarkable potency resolving inflammation-related diseases in animal models of periodontitis, asthma and colitis (for a review, see ref. 8). Since increasing dietary omega-3 fatty acids reduces obesity-associated complications (9–11), the purpose of this study was to test the hypothesis that RvD1 and RvD2 can attenuate adipose inflammation and investigated their production and conversion by adipose tissues.

MATERIALS AND METHODS

Mice

C57BL/6 mice with diet-induced obesity (60 kcal% high-fat up to 16 weeks) and control mice were from The Jackson Laboratory (Bar Harbor, ME). The high-fat model is a reproducible model of obesity and pre-type 2 diabetes and closely mirrors human obesity, most of which is thought to occur in response to high-fat intake (12). For the C57BL/6J strain, average % weight gain is typically about 43% at the 16th week of feeding and the variation among animals within the same diet group is less than 10%. Experiments were performed in accordance with the Harvard Medical School Standing Committee on Animals guidelines for animal care and approved protocol #02570.

Immunohistochemistry

Adipose tissue was fixed in 3.3% formalin, paraffin-embedded and sectioned at the Research Pathology Core of the Dana-Farber/Harvard Cancer Center (Boston, MA). Distribution of ALX/FPR2 receptor was detected using a rabbit anti-mouse ALX/FPR2 Ab (1/250) (Santa Cruz Biotechnology, Santa Cruz, CA). Color was developed using Vectastain ABC Kit (Vector Laboratories, Burlingame, CA) and sections were counterstained with hematoxylin. Distribution of ChemR23 was detected using a rat anti-mouse ChemR23 Ab labeled with PE (eBioscience, San Diego, CA). Sections were visualized at magnification X200 imaged with a Zeiss YFL microscope (Thornwood, NY) and ImagePro Plus 7 software (Media Cybernetics, Bethesda, MD).

[4]Abbreviations used in this paper: DHA, docosahexaenoic acid; EPA, eicosapentaenoic acid; EOR, eicosanoid oxidoreductase; LC-MS/MS, liquid chromatography tandem mass spectrometry; LM, lipid mediator; MRM, multiple reaction monitoring; Rv, resolvin; RvD1, Resolvin D1, 7*S*,8*R*,17*S*-trihydroxy-4*Z*,9*E*,11*E*,13*Z*,15*E*,19*Z*-docosahexaenoic acid; RvD2, Resolvin D2, 7*S*,16*R*,17*S*-trihydroxy-4*Z*,8*E*,10*Z*,12*E*,14*E*,19*Z*-docosahexaenoic acid; SPM, specialized pro-resolving mediators.

Adipose tissue explants and “ex vivo” incubations

Epididymal fat pads from obese mice were collected under sterile conditions and placed in a P60 plate with pre-warmed (37°C) DPBS containing penicillin (100 U/ml) and streptomycin (100 mg/ml). Connective tissue and blood vessels were removed by dissection before cutting the tissue into small pieces (<10 mg). Explants were cultured in DMEM with L-glutamine (2 mM), penicillin (50 U/ml), streptomycin (50 mg/ml) and 2% fatty acid free-BSA. Adipokine secretion and mRNA expression were assessed in explants incubated with vehicle (0.01% EtOH), rosiglitazone (0.3–10 μM), RvD1 (10 nM), RvD2 (10 nM), 17*R*-RvD1 (0.01–100 nM), LXA_4 (10 nM) or with equimolar concentrations (10 nM) of a mixture of RvD1, RvD2, 17*R*-RvD1 and LXA_4 for 4, 6, 12 and 24 h at 37°C. To assess RvD1, RvD2 and 17*R*-RvD1 metabolism by adipose tissue, incubations were initiated by adding 1 μg of the selected compound at 37°C for 0.5, 6 and 12 h. In some experiments, incubations were carried out in the presence of 100 μM of indomethacin or α-methylcinnamic acid. Incubations were stopped with cold methanol (2 vol) and samples were taken to C18 solid extraction and subjected to LC-MS/MS.

Isolation and culture of adipocytes

Mouse fat pads were excised, rinsed two times in cold carbogen-gassed (5% CO_2:95% O_2) Krebs Ringer and minced into fine pieces. Minced samples were placed in Krebs Ringer supplemented with 1% fatty acid-free BSA and 2 mM of EDTA and centrifuged at 500*g* for 5 min at 4°C to remove free erythrocytes and leukocytes. Tissue suspensions (1 g) were placed in 5 ml of Krebs Ringer buffer supplemented with 1% fatty acid-free BSA and 1 mg/ml of collagenase A and incubated at 37°C for 60 min with gentle shaking. Tissue homogenates were filtered through a 100 μm nylon mesh and then centrifuged at 500*g* for 5 min. Floating cells were collected, washed two times in carbogen-gassed DMEM supplemented with L-Glutamine (2 mM), penicillin (100 U/ml), streptomycin (100 mg/ml) and HEPES (100 mM) and suspended in this DMEM medium containing 0.2% endotoxin-free fatty acid-free BSA before counting and plating on 12-well or 96-well plates.

Lipid Mediator-Metabolo-lipidomics

LC-MS/MS based metabolo-lipidomics was performed using linear ion trap triple quadrupole mass spectrometer MS (3200 QTRAP, Applied Biosystems, Foster City, CA) equipped with two HPLC pumps (LC-20AD, Shimadzu, Kyoto, Japan) coupled to an Eclipse Plus C18 reverse phase column (4.6 mm × 50 mm × 1.8 mm, Agilent Technologies, Palo Alto, CA). The mobile phase consisted of MeOH:H_2O/acetic acid at a ratio of 60:40:0.01 (vol:vol:vol) and ramped to 80:20:0.01 after 10 min and to 100:0:0.01 after 12 min. Instrument control and data acquisition were performed using Analyst 1.5 software (Applied Biosystems). Ion pairs from reported MRM methods (13) were used for profiling and quantification of bioactive lipid mediators. Quantification was performed using standard calibration curves for each, and recoveries were calculated using deuterated internal standards (d4-LTB_4d4-PGE_2 and d8-5-HETE) purchased from Cayman Chemical (Ann Arbor, MI).

Enzymatic conversion

RvD1, RvD2 and 17*R*-RvD1 (100 ng) were taken to dryness under N_2 stream and incubated with recombinant human 15-PG-dehydrogenase/eicosanoid oxidoreductase (EOR) (0.5 U) (Cayman Chemical, Ann Harbor, MI) in 100 μl of Tris-HCl buffer (50 mM, pH 7.4) containing NAD^+ (1.0 mM). EOR activity was monitored spectrophotometrically by the formation of NADH from NAD^+ at 340 nm. Enzymatic conversion of RvD1, RvD2 and 17*R*-RvD1 (100 ng) was also tested in 100 μl incubations of Tris-HCl buffer (50 mM, pH 7.4) containing NADPH (0.1–0.5 mM) and 11β-hydroxysteroid dehydrogenase type 1 (2 U)

(Cayman Chemical). All incubations were allowed to proceed for 30 min at 37°C and stopped with cold methanol before C18 solid phase extraction for further analyses using LC/MS-MS.

Oxo-RvD2 products

RvD2 (1.5 mg) in ethanol was dried down under N_2 stream and suspended in buffer containing Tris-HCl (100 μl, 50 mM, pH 7.4) and NAD^+ (1.0 mM). Enzymatic conversion was initiated by the addition of recombinant human EOR (0.5 U) and allowed to proceed for 30 min at 37°C. After 30 min, reactions were stopped with cold methanol and taken for C18 solid phase extraction. oxo-containing products were isolated in a Hewlett-Packard 1100 Series HPLC system equipped with a Phenomenex Luna C18 (150×2 mm × 5 mm) column and a diode array detector. Products were eluted with MeOH/H_2O/acetic acid (70:30:0.01) as phase one (*t*0, −10 minutes), and a linear gradient with MeOH/acetic acid (99.9:0.1) as phase two (10–30 minutes), at a flow rate of 0.2 ml/min.

Adipokines and Cytokines

Adiponectin and leptin levels in supernatants from adipose tissue explants were quantified by EIA (Cayman Chemical). Concentrations of TNF-α, IL-6, IL-12, IL-10, IL-1β, IL-13, IL-33 and IL-4 were assessed by a custom-made Luminex multiplex cytokine-detection bead assay platform using a Luminex® 200™ instrument (Luminex Corp., Austin, TX). The assay was conducted using 20 μl of supernatants from adipose tissue explants. Data acquisition and analysis were conducted using StarStation software v2.3 (Applied Cytometry Systems, Dinnington, UK).

RNA isolation, reverse transcription and Real-Time PCR

Total RNA from adipose tissue was isolated using the TRIzol reagent. RNA concentration was assessed in a NanoDrop-1000 spectrophotometer (NanoDrop Technologies, Wilmington, DE). cDNA synthesis from 100–200 ng of total RNA was performed using the Omniscript kit (Qiagen, Hilden, Germany). Real-Time PCR was performed with validated and pre-designed QuantiTect® Primer Assays (Qiagen) for adiponectin (QT01048047) and EOR (QT01039192) or TaqMan® Gene Expression Assays for MCP-1 (Mm00441242_m1) using GAPDH (QT01192646) as endogenous control. Real-time PCR amplifications were carried out in an ABI 7900HT thermal cycler (Applied Biosystems). Relative quantification of gene expression was performed using the comparative C_t method. Conventional PCR amplification of mouse ChemR23 and ALX/FPR2 and human ChemR23, ALX/FPR2, GPR32 and GADPH was performed with specific primer pairs. PCR products were analyzed by electrophoresis in 2.0% agarose gels and visualized by ethidium bromide staining.

Monocyte-adipocyte assays

Murine bone marrow-derived monocytes were isolated using the EasySep® mouse monocyte-enrichment kit (StemCell Technologies, Vancouver, Canada). Following isolation, cells were counted and resuspended in PBS^{++} containing 0.1% BSA at a density of 2×10^6 cells/ml. Mouse adipocytes were isolated as described above and resuspended in DMEM at 0.9×10^6 cells/ml and 25,000 cells/well were loaded onto a 96-well ChemoTx® plate (Neuro Probe, Gaithersburg, MD) with polycarbonate membrane filters and 3-μm membrane pores which require modest amounts of testing compounds. Adipocytes were incubated for 1 h at 37°C, subsequently either LTB_4 (10 nM) or MCP-1 (15 ng/ml) was added to the lower wells and the isolated monocytes were then loaded on top of membrane in the presence of 10 nM of RvD1, RvD2, 17*R*-RvD1, 17(*R/S*)-methyl-RvD1 (from Dr. Nicos Petasis, University of Southern California, and prepared as in Kasuga et al. (14)) or the corresponding RvD1 and RvD2 oxo-containing products. Cells were then co-incubated

for 90 min at 37°C. The cells that did not transmigrate were washed whereas the transmigrated cells along with adipocytes were immunofluorescent-stained as detailed below. The number of transmigrated monocytes and the number of monocytes adhered to adipocytes were assessed by using a rabbit anti-perilipin polyclonal Ab (1 μg/ml) (Abcam, Cambridge, MA) in combination with a donkey anti-rabbit PE conjugated Ab and a rat anti-mouse CD11b or a mouse anti-human CD11b FITC conjugated Ab (eBioscience). Staining was assessed on a FACSCanto II flow cytometer using BD FACSDiva 4.1 software (Becton Dickinson, San Jose, CA). The number of transmigrated monocytes was calculated as a function of the number of CD11b-positive, perilipin-negative cells. Monocyte-adipocyte interactions were quantified by measuring CD11b levels in the perilipin-positive cells. In a separate set of experiments the chemotactic properties of RvD1, RvD2 and the oxo-containing RvD1 and RvD2 metabolites were assessed by loading the compounds in the bottom well of the ChemoTx® plates and loading the monocytes on top of the filter. Cells were then incubated for 90 min at 37°C and the number of transmigrated cells was assessed as above.

Human PBMC were isolated from healthy volunteer peripheral blood according to protocol #1999P001297 approved by the Partners Human Research Committee. Briefly, blood collected in heparin was centrifuged (200*g*) for 15 min removing the platelet-rich plasma fraction. Cells were then layered over Ficoll-Hypaque (Organon Teknika, Durham, NC) and centrifuged (500*g*) for 35 min. The mononuclear cell layer was collected, washed once, and resuspended in PBS containing 2% FCS and 1 mM EDTA. PBMC were then isolated using a human monocyte isolation kit (StemCell Technologies) and resuspended in PBS^{++} containing 0.1% BSA at a density of 2×10^6 cells/ml. Human subcutaneous fresh primary adipocytes (floaters) were obtained from obese individuals with a body mass index (BMI) ≥ 30 and age between 39 and 46 years (Zenbio, Research Triangle Park, NC) and grown in DMEM at a concentration of 2×10^6 cells/ml. Monocyte transmigration to the stimulated human adipocytes (25,000 cells/well) was assessed as outlined above for the mouse cells. Monocyte-adipocyte interactions were assessed by measuring the CD11b expression levels in the perilipin-positive cells.

RESULTS

First we compared endogenous biosynthesis of pro-resolving mediators in adipose tissues from lean and obese mice. Adipose tissues were subjected to LC-MS/MS-based lipid mediator metabolo-lipidomics (see Materials and Methods), and in profiles obtained from adipose tissue we identified RvD1 (7S,8R,17S-trihydroxy-4Z,9E,11E,13Z,15E,19Z-docosahexaenoic acid), RvD2 (7S,16R,17S-trihydroxy-4Z,8E,10Z,12E,14E,19Z-docosahexaenoic acid) and protectin D1 (PD1: 10R,17S-dihydroxy-4*Z*,7*Z*,11*E*,13*E*,15*Z*,19*Z*-docosahexaenoic acid) from endogenous sources in both lean and obese mice. Representative chromatograms of selected MRM (m/z 375>215, m/z 375>233, m/z 359>153) and representative tandem mass spectra for RvD1, RvD2 and PD1 are in Figure 1A–D. Compared to lean animals, adipose tissue from obese mice had reduced levels of both RvD1 and PD1 (Figure 1E). Also, levels of 17S-hydroxydocosahexaenoic acid (17-HDHA: 17S-hydroxy-4Z,7Z,10Z,13Z,15E,19Z-docosahexaenoic acid) and 18-hydroxyeicosapentaenoic acid (18-HEPE: 18R-hydroxy-5Z,8Z,11Z,14Z,16E-eicosapentaenoic acid), the monohydroxy markers of D-series and E-series resolvin biosynthesis, were significantly lower in fat from obese mice (Figure 1F). We also identified 14S-hydroxydocosahexaenoic acid (14-HDHA: 14S-hydroxy-4Z,7Z,10Z,12E,16Z,19Z-docosahexaenoic acid), a marker of maresin biosynthesis pathway including MaR1 (15) in these that was also decreased (Figure 1F).

Significant levels of eicosanoids derived from arachidonic acid, including 5-hydroxyeicosatetraenoic acid (5-HETE), 12-HETE, 15-HETE, PGE_2, PGD_2 and $PGF_{2\alpha}$, were also present in these tissues (Figure 2). Compared to lean, obese adipose gave increased 5-HETE with reduced PG as well as 12-HETE and 15-HETE levels (Figure 2).

To translate these findings, human adipocytes from obese patients were obtained and LM-metabololipidomics carried out. As shown in Figure 3 the profiles of LM identified in human adipocytes were similar to those obtained from mouse adipocytes. However, mouse adipocytes produced higher amounts of RvD1, PD1, 14-HDHA, 17-HDHA and 18-HEPE as well as 12-HETE and 15-HETE than human adipose (Figure 3). Conversely, human adipocytes produced higher PGE_2, PGD_2 and $PGF_{2\alpha}$ than mouse adipocytes (Figure 3) while the 5-LOX products 5-HETE, LTB_4 and LXA_4 were essentially similar in both species (Figure 3).

Do adipose tissues express receptors for specialized pro-resolving mediators (SPM)? To address this, adipose tissue from lean and obese mice were assessed for expression of ALX/FPR2 and ChemR23 receptors for RvD1 and RvE1, respectively (16). Representative PCR analysis of mRNA receptor expression and immunohistochemistry are in Figure 4A. In human cells RvD1 also signals *via* GPR32 (16), which apparently is not present in murine cells, a receptor that was found to be constitutively expressed in human subcutaneous fat in addition to ALX/FPR2 and ChemR23 receptors (Figure 4A). Hence, adipose tissue expresses the three presently known GPCR for RvD1, RvE1 and LXA_4.

To determine the functional relevance of RvD1 and RvD2 in inflamed adipose, we assessed their impact on adhesion of monocytes to adipocytes and monocyte transadipose migration, which are critical events in mounting a strong inflammatory response within obese adipose (4, 5). To this end, we used established cellular responses in a 96-well ChemoTX plate. These were performed by adding a chemotactic stimulus, either MCP-1 or LTB_4, to the bottom wells, with 25,000 adipocytes suspension below the membrane and 50,000 monocytes placed above the membrane in the presence of either RvD1 or RvD2. MCP-1 and LTB_4 were employed as monocyte chemoattractants since they were also increased in obese adipose tissue (Figure 4B and C). Of interest, the chemotactic responses to MCP-1 (15 ng/ml) were significantly higher in monocytes obtained from obese mice compared to those from lean mice (Figure 4E). Here, similar responses to LTB_4 (10 nM) were obtained (Figure 4D).

Addition of LTB_4 to the bottom wells caused increased monocyte attachment to adipocytes and transadipose migration that were markedly reduced by 10 nM of either RvD1 or RvD2 (Figure 4F). Similar inhibitory actions for RvD1 and RvD2 were obtained after addition of MCP-1 (Figure 4G). No synergic actions were observed after simultaneous addition of equimolar RvD1 and RvD2 (n=3). For purposes of direct comparison, RvD1 actions were compared with those obtained with 17*R*-RvD1 and its analog 17(*R/S*)-methyl-RvD1 (14), which resists rapid inactivation (Supplemental Figure 1). Of interest, the inhibitory actions of RvD1 at nanomolar concentrations with monocyte chemotaxis were superior in monocytes from lean mice compared to those from obese mice (Supplemental Figure 1). This suggests that obesity may activate circulating monocytes. To translate these findings, human adipocytes from obese patients were obtained and assessed as above. With human adipocytes and monocytes, we found that the inhibitory actions of RvD1, RvD2 and 17*R*-RvD1 (10 nM each) on MCP-1 and LTB_4-induced monocyte adhesion to adipocytes and transadipose migration were similar to those observed with mouse cells (Supplemental Figure 2A,B).

Adipose tissue inflammation and increased monocyte recruitment in obesity is accompanied by a dysregulated secretion of the anti-diabetic and anti-inflammatory adipokine adiponectin, which is an essential homeostatic factor for systemic energy metabolism and insulin sensitivity (2). Consistent with this, mRNA expression and protein levels of adiponectin were consistently reduced in adipose tissues from obese mice (Figure 5A). To explore whether SPM could rescue impaired adiponectin secretion in obesity, adipose tissue explants from obese mice were exposed to 10 nM of RvD1, RvD2, LXA_4 or 17*R*-RvD1 as well as a mixture of SPM (as might be encountered *in vivo*) and adiponectin levels were monitored (at 12 h, 37°C). Each SPM, including RvD1, RvD2, LXA_4 and 17*R*-RvD1, significantly increased adiponectin secretion (Figure 5B). In this regard, the SPM mixture was the most potent.

Of note, the levels of leptin in supernatants of adipose tissue explants gradually declined with treatment, reaching statistical significance with RvD2 alone and with the SPM mixture (Figure 5B). Next, we carried out concentration- and time-response experiments with 17*R*-RvD1, the SPM with the most potent actions on adiponectin. Incubation of adipose tissue explants with 17*R*-RvD1 increased adiponectin secretion in a concentration-dependent manner (Figure 5C). This concentration-response curve proved to be bell-shaped like other bioactive lipid mediators (17). Interestingly, 17*R*-RvD1 induced adiponectin to a similar extent to rosiglitazone, a known inducer of adiponectin production (18). However, the concentrations required for this thiazolidinedione were 1,000 times higher than those required for 17*R*-RvD1 (Figure 5C). Adiponectin gene regulation was assessed after 6 h of adipose tissue revealing that RvD1, 17*R*-RvD1 and RvD2 significantly induced gene expression to levels similar to those observed following rosiglitazone treatment that was 300 times the concentration of Rv (Figure 5D). The Rv precursor DHA at 10 nM did not induce adiponectin gene expression (n=3). At the protein level, up-regulation of adiponectin secretion by 17*R*-RvD1 and rosiglitazone peaked after 12 h (Figure 5D).

Another hallmark of obesity and insulin resistance is increased secretion of inflammatory cytokines, mainly IL-6 and TNF-α by adipose (2). To further assess the impact of resolvins on adipose tissue, cytokines were monitored after incubating fat explants with RvD1, RvD2 and 17*R*-RvD1. RvD1 drastically reduced levels of TNFα the pro-inflammatory and insulin-resistant adipokine (2), as well as IL-12 and IL-1β while enhancing secretion of IL-10, an anti-inflammatory cytokine (19) (Figure 6). With RvD1, the levels of IL-6, IL-33, IL-13 and IL-4 remained unchanged (Figure 6). RvD2 and 17*R*-RvD1 reduced TNFα, IL-1β and IL-12 as well as IL-6 levels (Figure 6). Together, these findings indicate that D-series resolvins have a unique role in dampening inflammation in adipose tissues.

Since local tissue inactivation of resolvins is a limiting step in their bioactions (20), we next examined whether adipose metabolically convert resolvins. LC-MS/MS profiling indicated that incubation of adipose tissue explants with RvD1, RvD2 or 17*R*-RvD1 resulted in their rapid loss (Figure 7A). Within 30 minutes there was ~70% loss of RvD1 (Figure 7A). In contrast, RvD2 and 17*R*-RvD1 were more resistant to conversion with ~70% of each remaining (Figure 7A). Since RvD1 is rapidly inactivated by 15-hydroxy/oxo-eicosanoid oxidoreductase (15-PGDH) and eicosanoid oxidoreductases (EORs) (20, 21), we next sought evidence for 15-PG-dehydrogenase/EOR expression in adipose tissue. As shown in Figure 7B, expression in adipose tissue uncovered a remarkable up-regulation of this oxidoreductase in obese mice. Interestingly, RvD1, RvD2 and 17*R*-RvD1 appeared to offer positive feedback regulation and increased EOR expression in adipose tissue explants to a similar extent as rosiglitazone, an established EOR inducer (Figure 7C).

Based on their constitutive expression and role in determining adipose tissue catabolic activities (22), we next assessed whether inhibition of either EOR or other dehydrogenases,

i.e. 11β-hydroxysteroid dehydrogenase (Table 1), impacts adipose tissue conversion of resolvins. To this end, we incubated adipose explants with resolvins in the presence of indomethacin, which along with inhibiting COX is also a potent EOR inhibitor (21), or α-methylcinnamic acid, an 11β-hydroxysteroid dehydrogenase inhibitor (23). Addition of indomethacin resulted in ≥ 55% inhibition of RvD1 conversion, and α-methylcinnamic acid gave ~35% inhibition (Figure 7D). These findings are also consistent with the notion that RvD1 is a substrate for both oxidoreductases. Indomethacin also blocked conversion of both RvD2 and 17*R*-RvD1 by ~30% and ~15%, respectively (Figure 7D).

Since 15-PG-dehydrogenase/EOR oxidizes alcohols to their respective ketones (oxo) as in the conversion of PGE_2 (24), we determined the structure of these RvD1 and RvD2 further metabolites. RvD1 is further converted to both 8-oxo-RvD1 and 17-oxo-RvD1 (20), whereas the potential single oxo-containing product from RvD2 was expected to be either 7-oxo-RvD2 or 16-oxo-RvD2 (Figure 8 A and B). Hence, we assessed conversion of RvD2 by EOR, and using RP-HPLC, RvD2 and its further metabolites were separated using their distinct chromatographic behavior and UV absorbance properties. RvD2 eluted from the RP-HPLC system at 19.3 min and the presence of a conjugated tetraene within RvD2 gave its characteristic triplet chromophore λ_{max}^{MeOH} 301 nm (Figure 8C). The main metabolite derived from RvD2 conversion by recombinant human EOR eluted at 24.5 minutes and contained a single broad UV absorbance peak at λ_{max}^{MeOH} = 351 nm (Figure 8C). This predominant further metabolic product of RvD2 was identified as 7-oxo-RvD2 employing LC-MS/MS and GC-MS-based analyses and it was established as the initial oxidation product of RvD2 in obese adipose tissue (F.G., J.C., J.D., Sungwhan F. Oh, and C.N.S., manuscript in preparation). These results indicate that adipose tissue rapidly converts RvD2 by dehydrogenation to 7-oxo-RvD2, and emphasize that RvD2 further metabolism is governed by the 15-hydroxy/oxo-eicosanoid oxidoreductase, a process that is common in the local conversion and inactivation of other LM including PGs, LTs and LXA_4 (24).

Next, each of the further metabolites of RvD1 and RvD2 were taken for direct comparisons of their bioactivity with that of the parent molecule. As shown in Figure 8 D and E, 8-oxo-RvD1 limited MCP-1-induced monocyte adhesion to adipocytes and transadipose migration, whilst 17-oxo-RvD1 did not reduce monocyte recruitment in a statistically significant manner. These are consistent with those for PMN infiltration *in vivo* in murine peritonitis (20). Importantly, the new 7-oxo-RvD2, the predominant further metabolic product of RvD2 in adipose tissue, was essentially as active as RvD2 (~90% the activity of RvD2) (Figure 8 F and G). In sharp contrast, 16-oxo-RvD2 was inactive. Of note, unlike MCP-1, monocytes showed no chemotactic response to RvD1, 8-oxo-RvD1, RvD2 or 7-oxo-RvD2 when these were added alone to the bottom wells for 90 min (Supplemental Figure 2C).

DISCUSSION

Results of the present studies provide evidence of a heightened pro-inflammatory phenotype along with a compromised capacity to produce local SPM in obese adipose tissue. The mechanism(s) by which obesity results in a chronic pro-inflammatory phenotype within the adipose tissues are incomplete. In this context, hypoxia is a key driven force of chronic inflammation. Indeed, in the setting of obesity an imbalance between the supply of and demand for oxygen in enlarged adipocytes causes tissue hypoxia and an increase in inflammatory adipokines (25). The resultant infiltration by macrophages and chronic low-grade inflammation promote, in turn, insulin resistance in adipose tissue (26).

In addition, the local tissue loss of pro-resolving mechanisms and mediators in inflammation such as SPM is critical and can contribute to obesity-linked inflammation and insulin resistance. Likely this results from the lack of intrinsic capacity of adipose to generate

appropriate endogenous “stop signals” and pro-resolving mediators for catabasis and the return to complete resolution (7, 27). A deficit in SPM in obese adipose tissue can be the consequence of the structural deficiency in the tissue content of omega-3 fatty acids, namely DHA and EPA, as substrates for SPM biosynthesis (28). Since our findings also provide evidence that 15-PG-dehydrogenase/eicosanoid oxidoreductase, a key enzyme in SPM further metabolic conversion, is markedly up-regulated in obese adipose tissue, the local loss of SPM in obesity may reflect accelerated tissue SPM conversion to inactive metabolites. Interestingly, this SPM deficiency in obesity appears to be a generalized defect in all metabolic tissues, because in addition to adipose, it is also present in liver and skeletal muscle (28). Taken together, these findings are consistent with the notion that unresolved unremitting chronic “low grade” inflammation in obese adipose tissue is the result of an inappropriate inflammatory response that remains uncontrolled.

A key finding of the current study is that each of the resolution agonists RvD1 and RvD2 rescue the impaired phenotype of obese adipose tissue by enhancing expression and secretion of adiponectin in parallel with decreasing the secretion of pro-inflammatory adipokines/cytokines including leptin, TNFα, IL-6 and IL-1β. Resolvins also reduced monocyte-adipocyte adhesion as well as monocyte transadipose migration, a likely key event in the return of inflamed adipose tissue to homeostasis. The actions of RvD1 and RvD2 were neither additive nor synergistic. Moreover, the present results establish that an individual member of the resolvin family, RvD2, is enzymatically further metabolized in adipose tissue *via* NAD^+-dependent dehydrogenation of the hydroxyl group at carbon 7 to form 7-oxo-RvD2. This novel 7-oxo-RvD2 metabolite retained the anti-inflammatory actions of RvD2 in reducing both monocyte adhesion and transmigration with adipocytes.

Of interest, results from several recent studies demonstrate that many metabolic functions are controlled by circadian rhythm proteins (29). Although the direct influence of circadian rhythms on SPM and endogenous mechanisms in the resolution of inflammation remains largely unexplored, the circadian release of glucocorticoids is known and their link to downstream anti-inflammatory and pro-resolution mediator annexin A1 facilitates the return to homeostasis (30). Along these lines, prostaglandin 15d-PGJ_2, which can display anti-inflammatory properties, has recently been identified as an entrainment factor aligned with circadian oscillations (31). In light of these findings, it is plausible that local biosynthesis of SPM is controlled in part by circadian as well as stress responses (32) in various organs and tissues.

In line with the organ- and tissue-protective actions of SPM (8), pro-resolving mediators such as RvD1 and RvD1 skew adipose tissue macrophages toward a unique pro-resolving phenotype, ameliorating the incidence of obesity-related metabolic disorders (33, 34). Hence, enhancing local SPM production in adipose tissue, specifically those of the D-series resolvins and protectins, could reduce the inflammatory tone of obese adipose tissues. In turn, the local reduction of adipose inflammation by pro-resolving mediators such as RvD1 and RvD2 may reduce the adverse systemic impact of metabolic syndromes.

Supplementary Material

Refer to Web version on PubMed Central for supplementary material.

Acknowledgments

We thank M.H. Small for assistance with the manuscript.

REFERENCES

1. Ferrante AW. Obesity-induced inflammation: a metabolic dialogue in the language of inflammation. J. Intern. Med. 2007; 262:408–414. [PubMed: 17875176]
2. Ouchi N, Parker JL, Lugus JJ, Walsh K. Adipokines in inflammation and metabolic disease. Nat. Rev. Immunol. 2011; 11:85–97. [PubMed: 21252989]
3. Hotamisligil GS. Inflammation and metabolic disorders. Nature. 2006; 444:860–867. [PubMed: 17167474]
4. Lumeng CN, Saltiel AR. Inflammatory links between obesity and metabolic disease. J. Clin. Invest. 2011; 121:2111–2117. [PubMed: 21633179]
5. Zeyda M, Stulnig TM. Adipose tissue macrophages. Immunol. Lett. 2007; 112:61–67. [PubMed: 17719095]
6. Weisberg SP, McCann D, Desai M, Rosenbaum M, Leibel RL, Ferrante AW Jr. Obesity is associated with macrophage accumulation in adipose tissue. J. Clin. Invest. 2003; 112:1796–1808. [PubMed: 14679176]
7. Serhan CN, Brain SD, Buckley CD, Gilroy DW, Haslett C, O'Neill LAJ, Perretti M, Rossi AG, Wallace JL. Resolution of inflammation: state of the art, definitions and terms. FASEB J. 2007; 21:325–332. [PubMed: 17267386]
8. Serhan CN. Resolution phases of inflammation: novel endogenous anti-inflammatory and pro-resolving lipid mediators and pathways. Annu. Rev. Immunol. 2007; 25:101–137. [PubMed: 17090225]
9. González-Périz A, Horrillo R, Ferré N, Gronert K, Dong B, Morán-Salvador E, Titos E, Martínez-Clemente M, López-Parra M, Arroyo V, Clària J. Obesity-induced insulin resistance and hepatic steatosis are alleviated by omega-3 fatty acids: a role for resolvins and protectins. FASEB J. 2009; 23:1946–1957. [PubMed: 19211925]
10. Todoric J, Löffler M, Huber J, Bilban M, Reimers M, Kadi A, Zeyda M, Waldhäusl W, Stulnig TM. Adipose tissue inflammation induced by high-fat diet in obese diabetic mice is prevented by n-3 polyunsaturated fatty acids. Diabetologia. 2006; 49:2109–2119. [PubMed: 16783472]
11. Ramel A, Martinez A, Kiely M, Morais G, Bandarra NM, Thorsdottir I. Beneficial effects of long-chain n-3 fatty acids included in an energy-restricted diet on insulin resistance in overweight and obese European young adults. Diabetologia. 2008; 5:1261–1268. [PubMed: 18491071]
12. Petro AE, Cotter J, Cooper DA, Peters JC, Surwit SJ, Surwit RS. Fat, carbohydrate, and calories in the development of diabetes and obesity in the C57BL/6J mouse. Metabolism. 2004; 53:454–457. [PubMed: 15045691]
13. Yang R, Chiang N, Oh SF, Serhan CN. Metabolomics-lipidomics of eicosanoids and docosanoids generated by phagocytes. Curr. Protoc. Immunol. 2011; 95:14.26.11–14.26.26.
14. Kasuga K, Yang R, Porter TF, Agrawal N, Petasis NA, Irimia D, Toner M, Serhan CN. Rapid appearance of resolvin precursors in inflammatory exudates: novel mechanisms in resolution. J. Immunol. 2008; 181:8677–8687. [PubMed: 19050288]
15. Serhan CN, Yang R, Martinod K, Kasuga K, Pillai PS, Porter TF, Oh SF, Spite M. Maresins: novel macrophage mediators with potent anti-inflammatory and pro-resolving actions. J. Exp. Med. 2009; 206:15–23. [PubMed: 19103881]
16. Krishnamoorthy S, Recchiuti A, Chiang N, Yacoubian S, Lee C-H, Yang R, Petasis NA, Serhan CN. Resolvin D1 binds human phagocytes with evidence for pro-resolving receptors. Proc. Natl. Acad. Sci. U.S.A. 2010; 107:1660–1665. [PubMed: 20080636]
17. Shimizu T. Lipid mediators in health and disease: enzymes and receptors as therapeutic targets for the regulation of immunity and inflammation. Annu. Rev. Pharmacol. Toxicol. 2009; 49:123–150. [PubMed: 18834304]
18. Quinn CE, Hamilton PK, Lockhart CJ, McVeigh GE. Thiazolidinediones: effects on insulin resistance and the cardiovascular system. Br. J. Pharmacol. 2008; 153:636–645. [PubMed: 17906687]
19. Bazzoni F, Tamassia N, Rossato M, Cassatella MA. Understanding the molecular mechanisms of the multifaceted IL-10-mediated anti-inflammatory response: lessons from neutrophils. Eur. J. Immunol. 2010; 40:2360–2368. [PubMed: 20549669]

20. Sun Y-P, Oh SF, Uddin J, Yang R, Gotlinger K, Campbell E, Colgan SP, Petasis NA, Serhan CN. Resolvin D1 and its aspirin-triggered 17*R* epimer: stereochemical assignments, anti-inflammatory properties and enzymatic inactivation. J. Biol. Chem. 2007; 282:9323–9334. [PubMed: 17244615]
21. Clish CB, Sun YP, Serhan CN. Identification of dual cyclooxygenase-eicosanoid oxidoreductase inhibitors: NSAIDs that inhibit PG-LX reductase/LTB(4) dehydrogenase. Biochem. Biophys. Res. Commun. 2001; 288:868–874. [PubMed: 11688989]
22. Tomlinson JW, Stewart PM. The functional consequences of 11beta-hydroxysteroid dehydrogenase expression in adipose tissue. Horm. Metab. 2002; 34:746–751.
23. Brozic P, Golob B, Gomboc N, Rizner TL, Gobec S. Cinnamic acids as new inhibitors of 17beta-hydroxysteroid dehydrogenase type 5 (AKR1C3). Mol. Cell. Endocrinol. 2006; 248:233–235. [PubMed: 16337332]
24. Tai HH, Ensor CM, Tong M, Zhou H, Yan F. Prostaglandin catabolizing enzymes. Prostaglandins Oth. Lipid Mediat. 2002; 68–69:483–493.
25. Eltzschig HK, Carmeliet P. Hypoxia and inflammation. N. Engl. J. Med. 2011; 364:656–665. [PubMed: 21323543]
26. Ye J. Emerging role of adipose tissue hypoxia in obesity and insulin resistance. Int. J. Obes. (Lond.). 2009; 33:54–66. [PubMed: 19050672]
27. Serhan CN. A search for endogenous mechanisms of anti-inflammation uncovers novel chemical mediators: missing links to resolution. Histochem. Cell Biol. 2004; 122:305–321. [PubMed: 15322859]
28. White PJ, Arita M, Taguchi R, Kang JX, Marette A. Transgenic restoration of long-chain n-3 fatty acids in insulin target tissues improves resolution capacity and alleviates obesity-linked inflammation and insulin resistance in high-fat-fed mice. Diabetes. 2010; 59:3066–3073. [PubMed: 20841610]
29. Eckle T, Hartmann K, Bonney S, Reithel S, Mittelbronn M, Walker LA, Lowes BD, Han J, Borchers CH, Buttrick PM, Kominsky DJ, Colgan SP, Eltzschig HK. Adora2b-elicited Per2 stabilization promotes a HIF-dependent metabolic switch crucial for myocardial adaptation to ischemia. Nat. Med. 2012; 18:774–782. [PubMed: 22504483]
30. Perretti M, D'Acquisto F. Annexin A1 and glucocorticoids as effectors of the resolution of inflammation. Nat. Rev. Immunol. 2009; 9:62–70. [PubMed: 19104500]
31. Nakahata Y, Akashi M, Trcka D, Yasuda A, Takumi T. The in vitro real-time oscillation monitoring system identifies potential entrainment factors for circadian clocks. BMC Mol. Biol. 2006; 7:5. [PubMed: 16483373]
32. Csermely, P.; Korcsmáros, T.; Sulyok, K. Stress Responses in Biology and Medicine: Stress of Life in Molecules, Cells, Organisms, and Psychosocial Communities. Boston: Blackwell Publishing; 2007.
33. Titos E, Rius B, González-Périz A, López-Vicario C, Morán-Salvador E, Martínez-Clemente M, Arroyo V, Clária J. Resolvin D1 and its precursor docosahexaenoic acid promote resolution of adipose tissue inflammation by elicitying macrophage polarization toward a pro-resolving phenotype. J. Immunol. 2011; 187:5408–5418. [PubMed: 22013115]
34. Hellmann J, Tang Y, Kosuri M, Bhatnagar A, Spite M. Resolvin D1 decreases adipose tissue macrophage accumulation and imiproves insulin sensitivity in obese-diabetic mice. FASEB J. 2011; 25:2399–2407. [PubMed: 21478260]

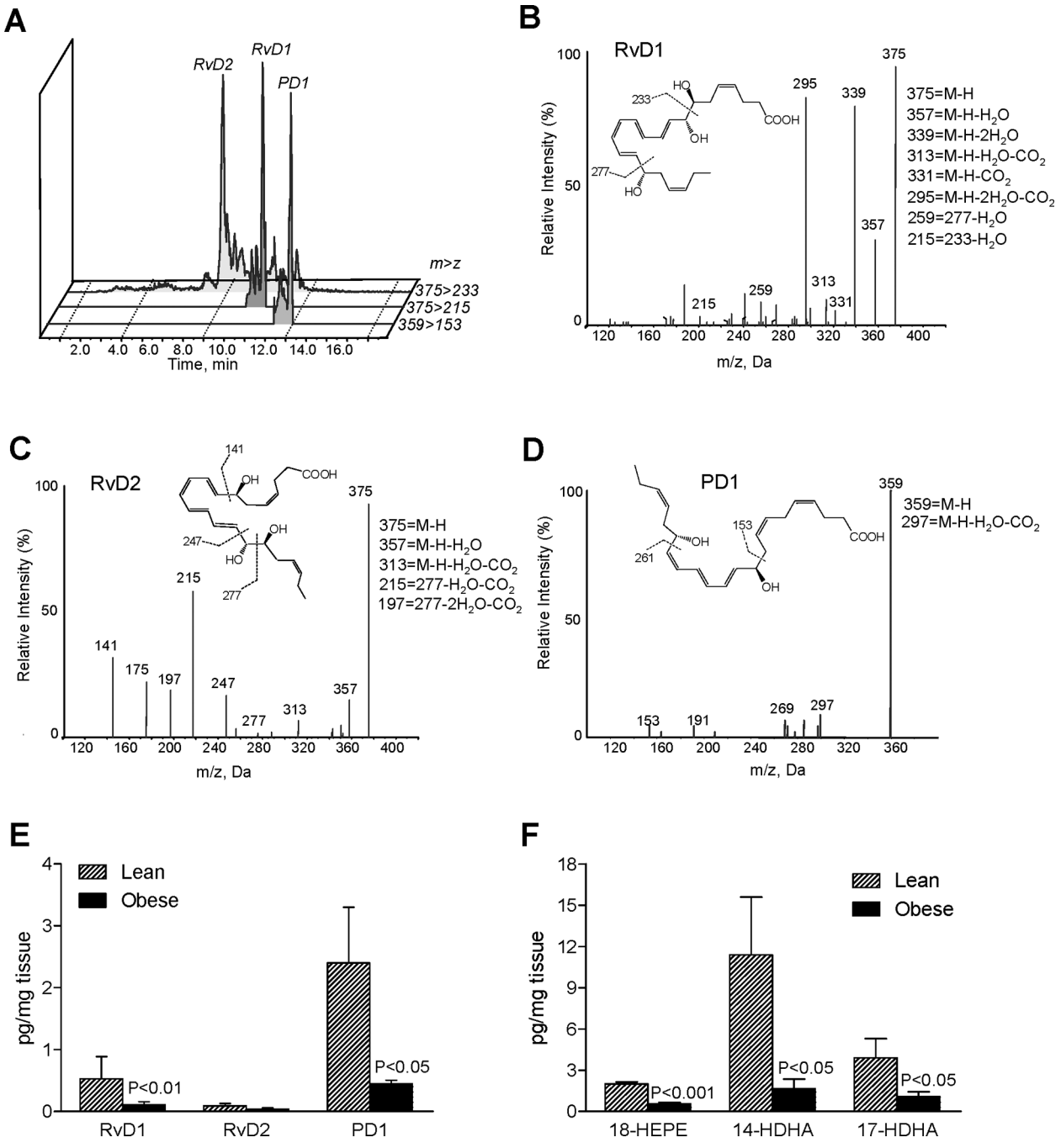

Figure 1. Specialized pro-resolving mediators (SPM) in obese adipose tissue: LC-MS/MS-based lipid mediator metabolo-lipidomics

(**A**) MRM chromatograms (m/z 375>233, 375>215 and 359>153) and representative tandem mass spectra of resolvin D1 (RvD1) (**B**), RvD2 (**C**) and protectin D1 (PD1) (**D**) in adipose tissue from obese mice. (**E**) Quantitation of SPM in adipose tissue from lean and obese mice. (**F**) Quantitation of monohydroxy markers of RvE1 and RvD1 biosynthetic pathways from EPA and DHA in adipose tissue from lean and obese mice. Results represent the mean ±SEM of 5 different individuals.

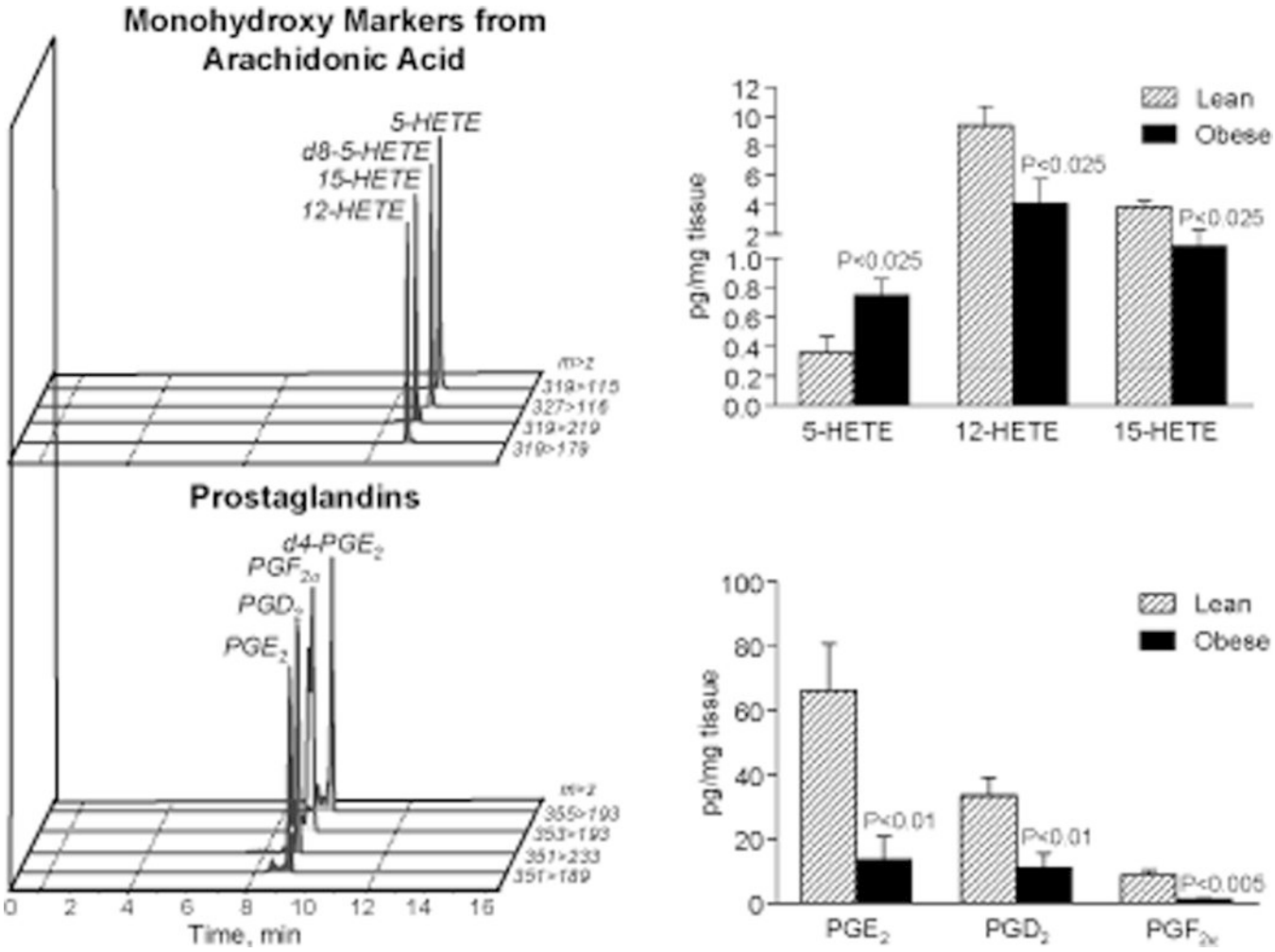

Figure 2. LC-MS/MS based metabolo-lipidomics of lipid mediators derived from arachidonic acid in obese adipose tissue

Representative MRM chromatograms of monohydroxy markers from arachidonic acid and prostaglandins (PGs) (*left panels*) and their quantitation in adipose tissue from lean and obese mice (*right panels*). Results represent the mean±SEM of 5 different individuals.

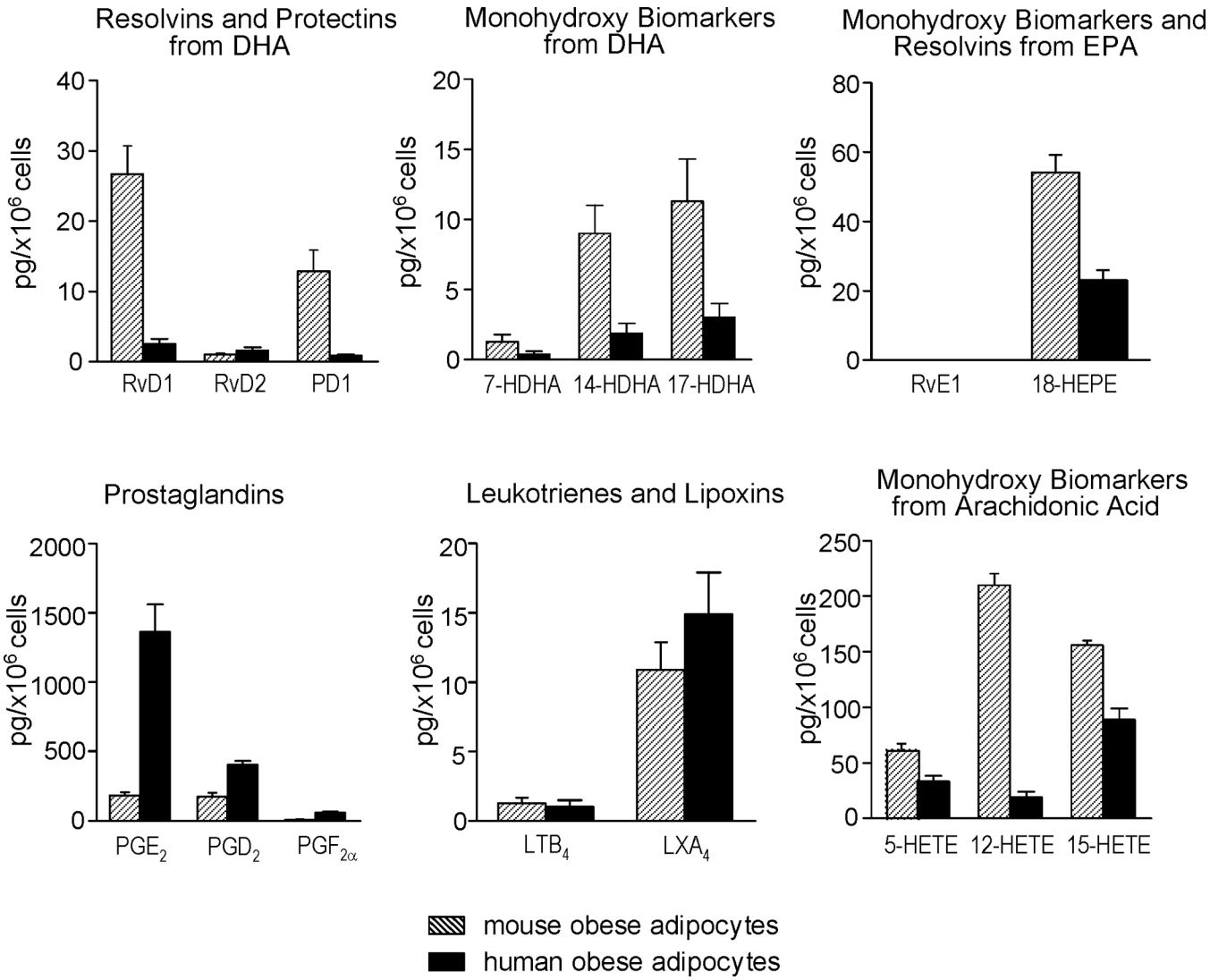

Figure 3. Specialized pro-resolving mediators (SPM) and eicosanoids in human and mouse adipocytes: LC-MS/MS-based lipid mediator metabolo-lipidomics

Quantitation of indicated lipid mediators in adipocytes isolated from epididymal fat pads of obese mice (shadowed bars) and adipocytes isolated from obese human subcutaneous fat samples (solid bars). Each compound was expressed as the quantity in picograms (pg) relative to 1×10^6 cells. Results are the mean±SEM of 3 different individuals.

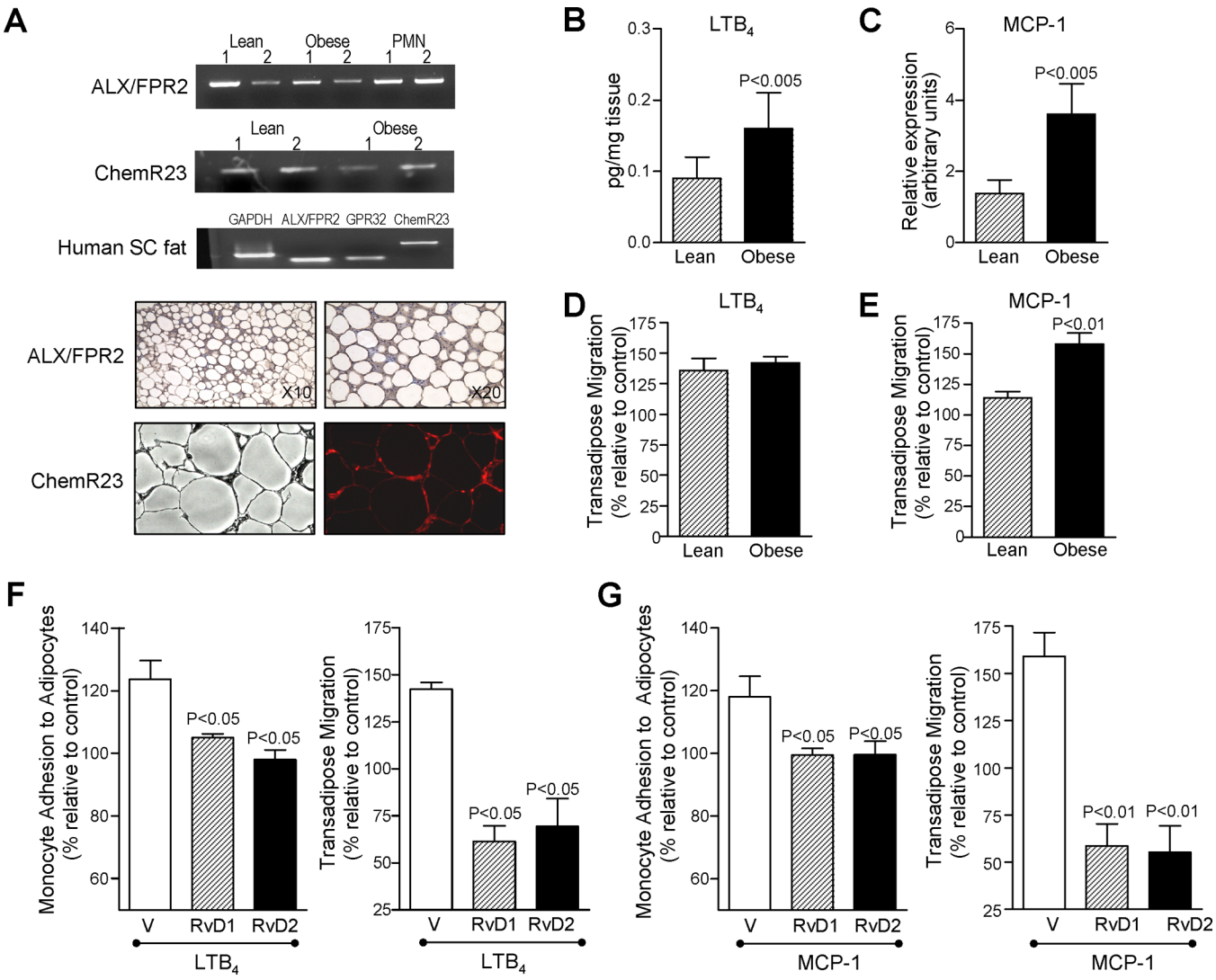

Figure 4. Pro-resolving mediator GPC receptors in adipose tissue and RvD1 and RvD2 attenuation of monocyte adhesion to adipocytes and transadipose migration

(**A**) Representative PCR analysis of ALX/FPR2 and ChemR23 receptors in adipose tissue from lean and obese mice (*upper panels*); representative expression of ALX/FPR2, GPR32 and ChemR23 receptors in human subcutaneous fat (*middle panel*); and representative photomicrographs of ALX/FPR2 and ChemR23 distribution in adipose tissue sections stained with either a primary rabbit anti-mouse ALX/FPR2 antibody or a rat anti-mouse ChemR23 antibody labeled with phycoerythrin (*lower panels*). RNA from mouse PMN was used as positive control for ALX/FPR2 expression. (**B**) LTB_4 levels in adipose tissue from lean and obese mice. (**C**) MCP-1 mRNA expression in adipose tissue from lean and obese mice. (**D,E**) Transadipose migration of monocytes from lean and obese mice in response to LTB_4 (10 nM) (**E**) and MCP-1 (15 ng/ml) (**E**). Murine adipocytes were loaded onto a 96-well ChemoTx® plate and LTB_4 or MCP-1 was added in the lower wells. Monocytes were placed on top of 3-μm-pore filters and co-incubated (90 min, 37°C). The number of transmigrated monocytes was assessed by flow cytometry using anti-CD11b antibodies. (**F,G**) RvD1 and RvD2 actions on obese monocyte interactions with adipocytes. Murine adipocytes were loaded onto a 96-well ChemoTx® plate and LTB_4 (10 nM) (**F**) or MCP-1 (15 ng/ml) (**G**) was added in the lower wells. Monocytes were placed on top in the presence

of 10 nM RvD1 or RvD2 and co-incubated (90 min at 37°C; see Materials and Methods). Results are the mean±SEM of 3 experiments in triplicate.

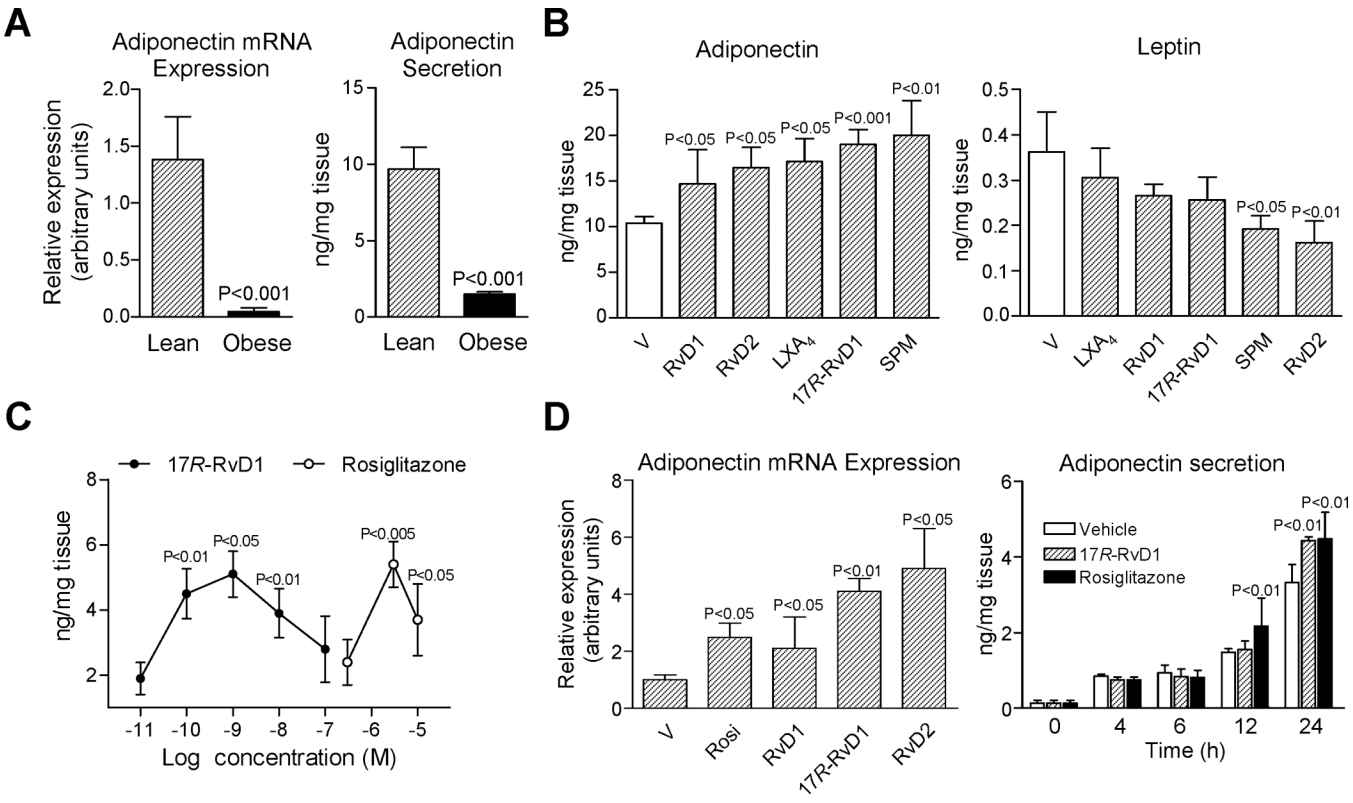

Figure 5. RvD1 and RvD2 potently induce adiponectin expression and secretion

(**A**) mRNA expression and tissue levels of adiponectin in fat from lean and obese mice. (**B**) Adipose tissue explants were incubated *ex vivo* with vehicle (0.01% EtOH) or 10 nM RvD1, RvD2, LXA_4 or 17*R*-RvD1 and a mixture of SPM (see text for details; 12 h at 37°C). Adiponectin and leptin levels in supernatants were quantitated by EIA. (**C**) Concentration-response curves for 17*R*-RvD1 (0.01–100 nM) and rosiglitazone (0.3–10 μM) on adiponectin secretion. (**D**) Changes in adiponectin expression in adipose tissue after 6 h of treatment with rosiglitazone (rosi, 3 μM) and equiconcentrations (10 nM) of RvD1, 17*R*-RvD1 and RvD2 (*left panel*); and time-response for 17*R*-RvD1 (10 nM) and rosiglitazone (3 μM) (*right panel*). Results are the mean±SEM of 5 separate experiments.

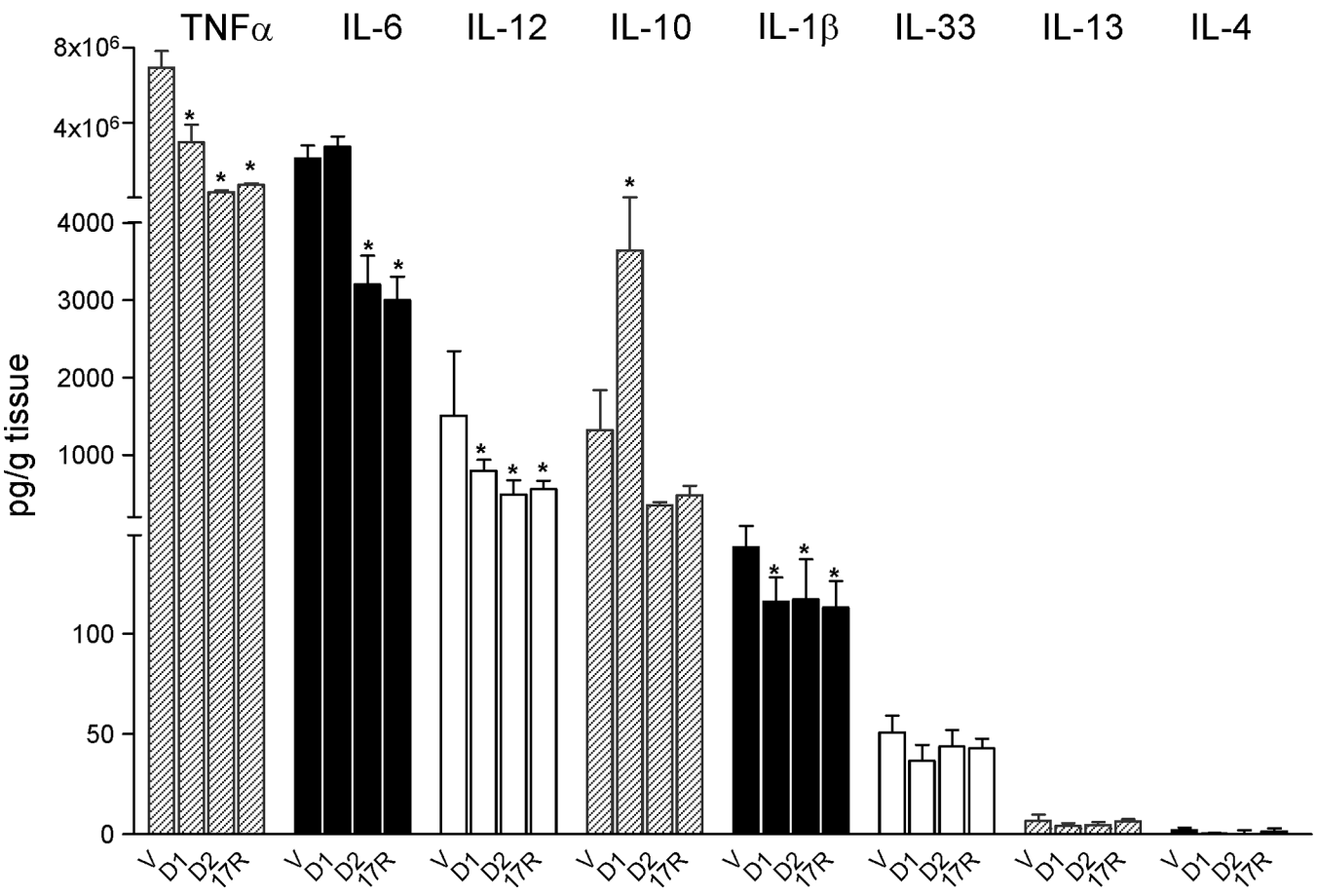

Figure 6. RvD1 and RvD2 reduce adipose tissue cytokine release

Cytokines measurements following addition of RvD1 (D1), RvD2 (D2) or 17*R*-RvD1 (17R) (10 nM, 12 h) were carried out using Luminex® cytokine multiplex. Results represent the mean±SEM of 3 experiments in duplicate. *, *P<0.05* versus vehicle (V).

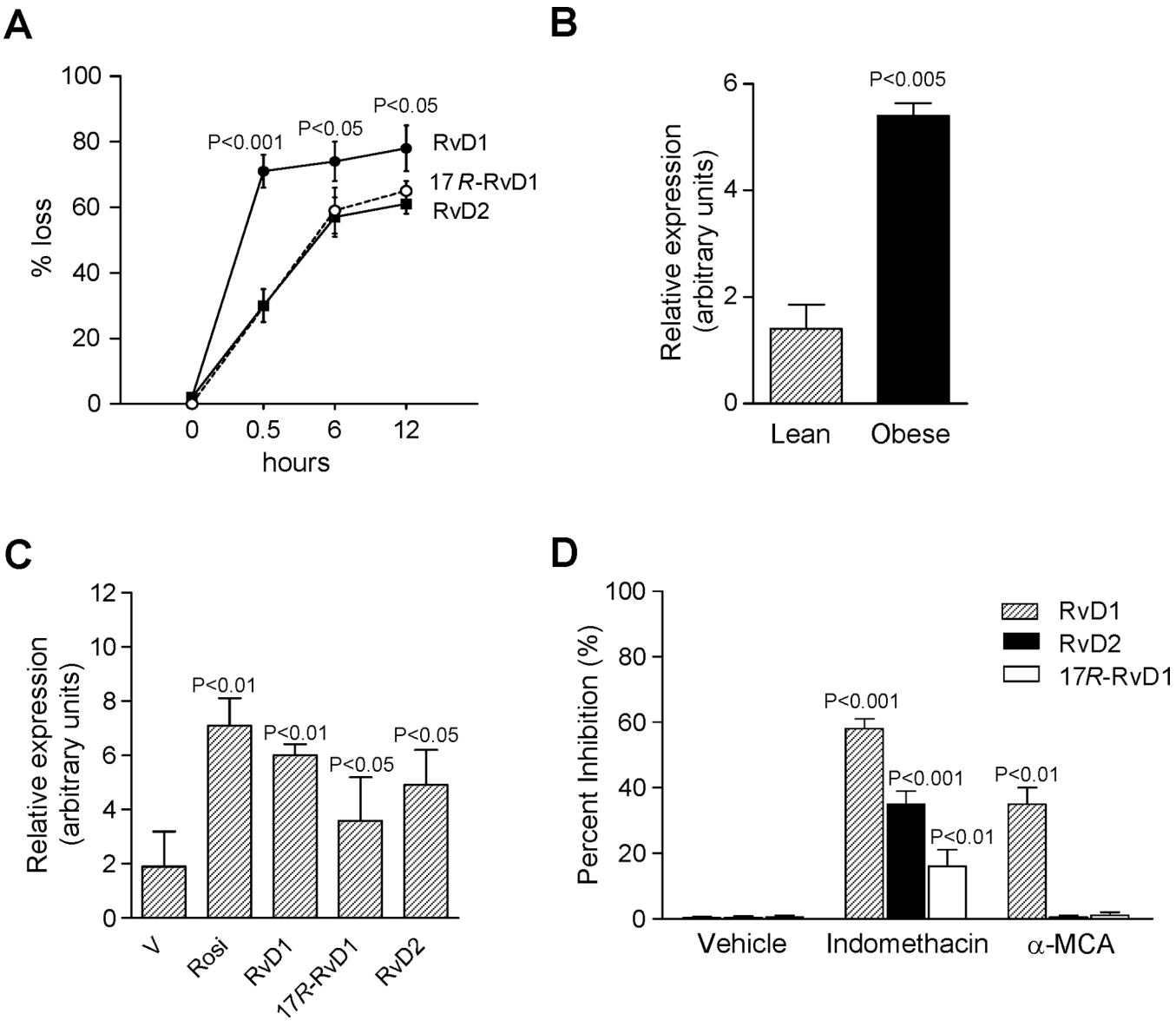

Figure 7. Rapid adipose tissue conversion of RvD1 and RvD2

(**A**) Time-course of conversion by adipose tissue. RvD1, 17*R*-RvD1 and RvD2 were each added to fat explants, and incubations (37°C) were stopped with cold methanol (2 vol) at the indicated time intervals, extracted and taken for LC-MS/MS. (**B**) mRNA expression for eicosanoid oxidoreductase (EOR) in adipose tissue from lean and obese mice. (**C**) Up-regulation of EOR in response to rosiglitazone (rosi, 3 μM), RvD1, RvD2 and 17*R*-RvD1 (10 nM each) treatment. (**D**) Inhibition of adipose tissue conversion of RvD1, RvD2 or 17*R*-RvD1 by indomethacin (indo, EOR inhibitor, 100 μM) and α-methylcinnamic acid (α-MCA, 11β-hydroxysteroid dehydrogenase type 1 inhibitor, 100 μM). RvD1, RvD2 and 17*R*-RvD1 were added to fat explants in the absence or presence of inhibitors and 12 h later, incubations were stopped and extracted. Results are the mean±SEM of 4 separate experiments.

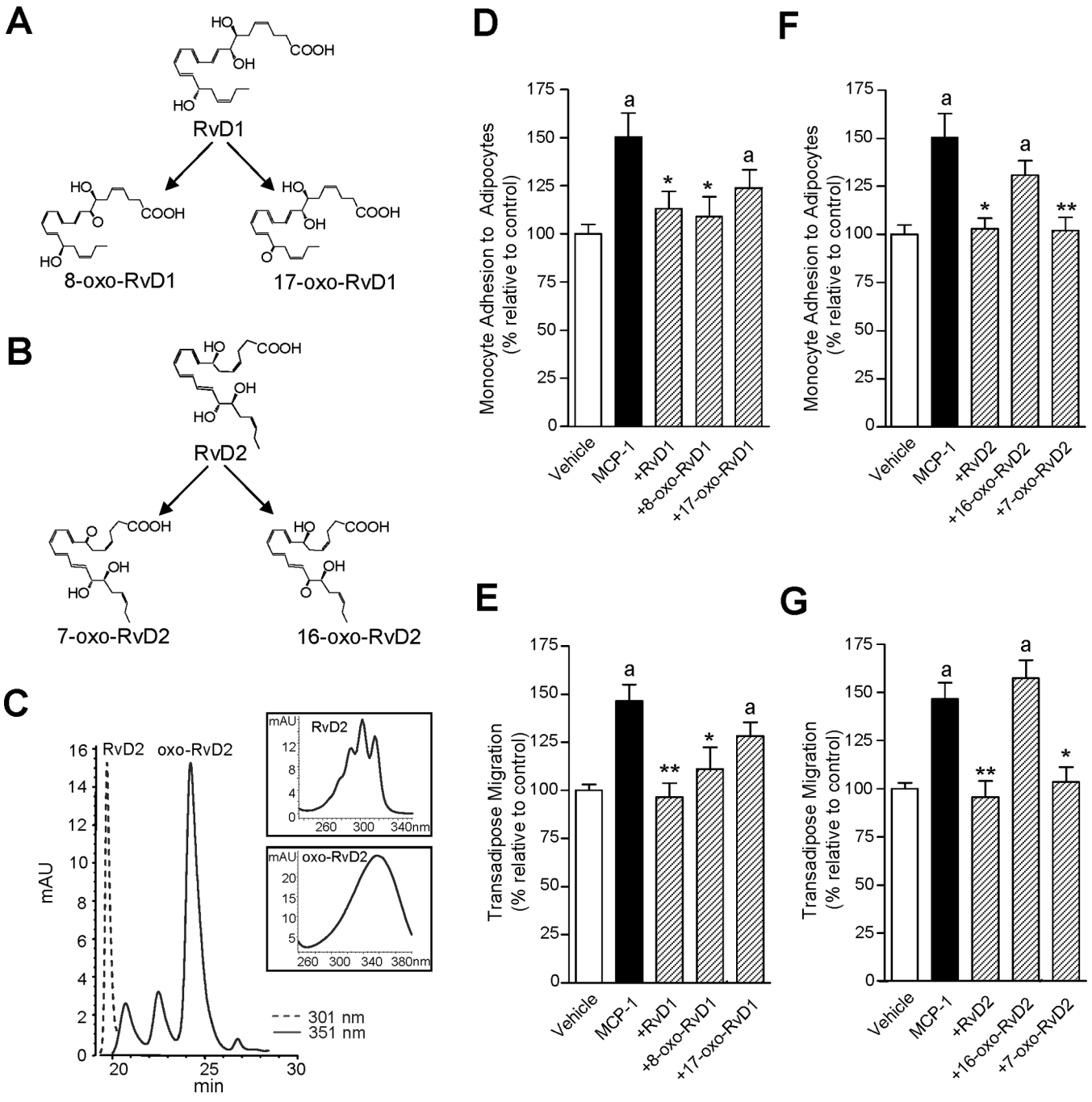

Figure 8. RvD2 conversion via 15-hydroxy/oxo-eicosanoid oxidoreductase and actions of novel Rv metabolites on monocyte-adipocyte interactions

(**A**) The initial step in RvD1 conversion is dehydrogenation to yield 8-oxo-RvD1 or 17-oxo-RvD1. (**B**) Conversion of RvD2 by dehydrogenation to yield 7-oxo-RvD2 or 16-oxo-RvD2. (**C**) HPLC chromatogram of RvD2 (λ_{max}^{MeOH} = 301 (*dotted line*)) and novel oxo-RvD2 metabolites (λ_{max}^{MeOH} = 351 (*solid line*)) generated by the incubation of RvD2 (1.5 mg) with recombinant EOR (0.5 U, 0.1 M Tris-HCl, 1 mM NAD^+, pH 7.4) for 30 min at 37°C. **Inset.** UV absorbance of RvD2 and the major oxo-containing peak eluting at 24.5 minutes. (**D–G**) Number of monocytes adhered to adipocytes and number of transmigrated monocytes in response to MCP-1 (15 ng/ml) in the presence of RvD1 metabolites (8-–oxo-

RvD1 and 17-oxo-RvD1) (**D,E**) and RvD2 metabolites (7-oxo-RvD2 and 16-oxo-RvD2) (**F,G**). The new RvD1- and RvD2-derived metabolites were produced using recombinant 15-hydroxy/oxo-eicosanoid oxidoreductase (15-PGDH), separated by RP-HPLC, extracted and tested. Results are the mean±SEM; n=3 assayed in triplicate. *, $P<0.05$ and **, $P<0.01$ versus cells exposed to MCP-1 alone. *a*, $P<0.05$ versus untreated vehicle.

Table 1

Resolvin D1 (RvD1), Resolvin D2 (RvD2) and 17*R*-RvD1 conversion by oxidoreductases.

	% Conversion		
	RvD1	**RvD2**	**17*R*-RvD1**
15-PG-dehydrogenase/Eicosanoid Oxidoreductase	68±10%	48±5%	20±8%
11β-Hydroxysteroid Dehydrogenase	18±3%	0±0%	0±0%

RvD1, RvD2 and 17*R*-RvD1 (100 ng) were incubated with recombinant human eicosanoid oxidoreductase (0.5 U) or recombinant human 11β-hydroxysteroid dehydrogenase type 1 (2.5 U) for 30 min at 37 °C. Reactions were stopped with 2 volumes of cold methanol and solid phase extracted and taken for LC-MS/MS (see Materials and Methods).